Unsupervised Structural Damage Assessment from Space using the Segment Anything Model (USDA-SAM): A Case Study of the 2023 Türkiye Earthquake

Sudharshan Balaji, Oktay Karakuş

Abstract

This paper explores advanced deep learning methods, specifically utilising the Segment Anything Model (SAM) along with image processing techniques, to evaluate the structural damages caused by the devastating earthquake that occurred in Turkey on February 6, 2023. Leveraging exceptionally high-resolution pre- and post-disaster imagery provided by Maxar Technologies, this paper showcases the efficacy of SAM in contrasting and quantifying the magnitude of structural devastation. The proposed *unsupervised structural damage assessment* (USDA-SAM) method entails a thorough comparative analysis of aerial imagery captured both before and after the seismic event, facilitating a nuanced evaluation of its impact on buildings and critical infrastructure. USDA-SAM also proposes two metrics - *damage assessment score* (DAS) and *affected number of buildings* (N_{b/km^2}) - to quantitatively measure the damage caused by the disasters. The study highlights the transformative potential of deep learning and image processing, shedding light on their key role in fortifying disaster response strategies and emphasising technology's indispensable contribution to mitigating the challenges posed by natural disasters, such as earthquakes.

Index Terms

Building detection, SAM, Segment Anything Model, Damage assessment

S. Balaji and O. Karakuş was with the School of Computer Science and Informatics, Cardiff University, Abacws, Senghennydd Road, Cardiff, UK.

NOTE: this is a non-peer reviewed preprint

I. INTRODUCTION

This paper highlights the significance of swift and precise damage assessment facilitated by the integration of Earth observation systems and artificial intelligence (AI) in response to natural disasters like earthquakes and floods. In 2023, the occurrence of severe floods in Libya and earthquakes in Türkiye and Syria emphasizes the urgent need for effective strategies in evaluating the damage caused by natural disasters. The impact of the 7.8 magnitude earthquake in Türkiye on February 6, 2023, and its subsequent 7.7 magnitude aftershock emphasized the necessity for robust preparedness measures. Efficiently monitoring the progression of destruction and assessing the scale of damage is crucial for directing rescue operations strategically and planning reconstruction efforts and rehabilitation of structures.

The seismic assessment landscape has evolved significantly, as evidenced by historical seismic damage detection methodologies. Early approaches in the 1970s and 1980s heavily relied on conventional techniques such as field surveys and aerial photography [1]–[3]. A paradigm shift occurred in the 1990s with the integration of satellite imagery and Geographic Information Systems (GIS). High-resolution earth observation satellites like Landsat 5 and SPOT played a pivotal role, enabling swifter and more detailed analyses of earthquake damage from a spatial perspective [4], [5].

The subsequent emergence of synthetic aperture radar (SAR) and interferometric SAR (InSAR) ushered in a new era, significantly enhancing post-disaster assessments. SAR's capabilities have been extensively documented, including three-dimensional reconstructions, cloud penetration, and independence from lighting conditions. InSAR, with its ability to compare SAR images over time, has proven invaluable for detecting subtle ground alterations in seismic zones [6], [7].

The early years of the 2000s witnessed a prevalence of computational imaging methods in remote sensing for earthquake damage assessment, primarily driven by the introduction of high-resolution satellites during this period. SAR imagery remained a prominent standard in the literature, complemented by the emerging inclusion of optical multi-spectral imagery. Throughout this decade, pixel-wise classification, building signature detection, edge/boundary detection and change detection techniques stood out as the predominant image processing methods [8]–[11].

Over the past fifteen years, there has been a surge in the exploration of artificial intelligence (AI) methods and the creation of foundational models capable of adeptly handling diverse tasks with remarkably high efficacy. Notably, advancements in computer vision research have significantly impacted studies in remote sensing for disaster surveillance, where the amalgamation of remote sensing imagery and AI techniques has proven influential. Presently, deep/machine learning techniques dominate this field of research, markedly enhancing conventional image processing methods like image fusion and multi-

modal data analysis through the incorporation of newly developed high-resolution remote sensing imagery [12]–[18].

Introduced by Meta AI in 2019 [19], the Segment Anything Model (SAM) has significantly transformed computer vision, particularly in instance segmentation, the task of identifying and segmenting diverse objects within images, even under partial obscuration. The recent implementation by Kirillov et al. [19] has further enhanced SAM's capabilities, revolutionising an initially challenging task plagued by inaccuracies. SAM's impressive performance stems from its sophisticated neural network architecture, trained on an extensive dataset of 11 million images with over 1 billion masks. This training enables SAM to excel in recognising intricate patterns and precise object segmentation. The model's potential applications span various fields, including medical imaging [20], [21] and remote sensing imagery [22], [23]. SAM's versatility offers evident benefits, such as flexibility and efficiency, eliminating the need for multiple specialised models and resulting in cost savings in computational resources and training time.

This paper investigates the utilisation of image segmentation methods for analysing satellite imagery to discern damage resulting from the devastating earthquake in Türkiye in 2023. The study is centred on a high-resolution dataset encompassing pre- and post-earthquake images made available by Maxar Technologies [24]. The primary aim is to develop an unsupervised approach for detecting and quantifying damage by examining masks derived from segmenting images through the Segment Everything Model (SAM) [19] pre-trained by a diverse array of annotated images and masks depicting various objects and structures. The *unsupervised structural damage assessment* (USDA-SAM) method involves several steps: extracting specific regions of interest from satellite images based on the earthquake's epicentre and affected zones, employing segmentation models trained on the Everything Prompt [19] dataset to generate masks representing distinct objects and structures in cropped images, and postprocessing the masks to enhance clarity while applying a coloured overlay to highlight damaged areas in map visualisation. In addition to visual assessment outcomes, the USDA-SAM technique also proposes two novel metrics named *damage assessment score* (DAS) and *the number of affected buildings* ($N_{\text{buildings}}$) to quantitatively evaluate the devastating damage caused by the disasters. By integrating these steps, a comprehensive evaluation of damage is possible through satellite imagery, offering valuable insights for rapid disaster response and optimal resource allocation.

II. Segment Anything Model (SAM)

The Segment Anything Model (SAM) [19] is a groundbreaking advancement in computer vision, excelling in image segmentation across diverse objects. Unlike traditional models confined to predefined categories, SAM's versatility allows it to operate on images of various fields, including autonomous

vehicles, augmented reality, medical diagnostics, and remote sensing. SAM's training involves a complex and data-intensive methodology, utilising a diverse dataset with images from various sources to enhance its adaptability in real-world scenarios. Masks in the SAM context are binary images precisely marking pixels belonging to an object against the background, crucial for the model to discern and understand spatial and structural characteristics.

SAM's architecture integrates state-of-the-art neural network designs, adept at processing visual information from images and masks, training to extract features, and continually improving accuracy and efficiency through extensive fine-tuning. Image segmentation is the intricate process of dividing a digital image into distinct segments, crucial for simplifying and enhancing the analysis of an image by assigning labels to pixels based on shared characteristics like colour, intensity, or texture, with the ultimate goal of identifying and isolating significant regions.

The Python package is known as *samgeo* [25], an adaptation of the *segment-anything-eo* repository, streamlines the integration of SAM for geospatial data analysis; nonetheless, its computational demands can be substantial. To address this, Zhao et al. [26] have introduced a computationally lighter version, *fast_sam*, utilising CNN architectures instead of transformers while maintaining comparable performance. Given the computational considerations, our building damage assessment in this paper employed the *fast_sam* approach.

III. Data & Pre-processing

The data utilised in this study was provided through the Open Data Program of Maxar Technologies, encompassing a dataset of 1,614 very-high-resolution RGB band satellite images capturing regions both pre- and post-impact by the 2023 Turkiye Earthquake. Predominantly focusing on forest and terrain areas, only approximately 2% of the images depict urban environments. The dataset includes imagery of affected cities such as Adiyaman, Hatay, Islahiye, K. Maras, and certain regions in Syria. Each of the 1,614 images is sized at 17,408 by 17,408 pixels.

We first conducted an exploratory analysis to examine pairs of images before and after the event. It is essential to have at least one pre/post pair for a given Region of Interest (RoI) to measure disparities in building distributions and evaluate structural damage in that specific area. Our analysis revealed that only 149 had both pre- and post-event image pairs, with a collection of 364 and 309 images, respectively (several RoIs have more than one pair). As previously indicated, the majority of these images originate from non-urban landscapes, a subset excluded from consideration in this paper. Our attention is directed solely towards the city centre and densely urbanised regions, leading to the selection of 9 RoIs encompassing areas of K. Maras, Osmaniye, Hatay and Islahiye. Finally, to facilitate computational

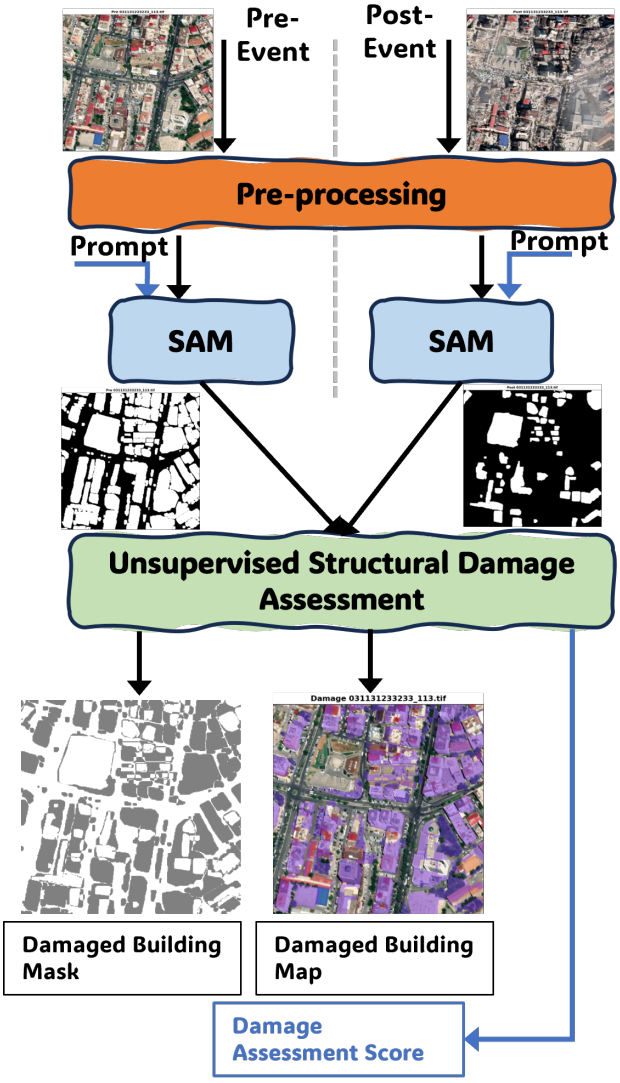

Fig. 1. Flowchart of the proposed USDA-SAM framework.

efficiency, each 17408 x 17408 satellite image has been divided into patches of equal size, resulting in 64 smaller patches.

IV. USDA-SAM

This paper concentrates on creating an unsupervised method for detecting and evaluating structural damage where we introduce the USDA-SAM, leveraging a high-resolution satellite imagery dataset captured before and after the earthquake. The specifics of the USDA-SAM method are illustrated in Figure 1.

After the data preprocessing phase, both pre and post-event images are inputted into the SAM model using the *everything prompt* and *fast_sam* Python packages. The proposed USDA-SAM method initially

generates building masks for each provided image, where objects identified are depicted in white against a black background, facilitating straightforward identification and analysis of changes. The discrepancy in masks between pre- and post-events is crucial for detecting earthquake-induced changes, which may manifest as alterations in the shape or size of the white areas, or in some cases, the complete disappearance of these areas, signifying substantial damage.

The masks generated by SAM exhibit various artefacts that could significantly impact the building damage analysis process. Consequently, we introduce a post-processing step before proceeding to the generation of damage masks and maps. This involved the removal of both small and large contours from the masks, under the assumption that they do not represent a distinctive building signature. Given SAM's tendency to produce numerous very small objects, we implemented a statistical elimination step, retaining only contours with areas falling between the 50% and 99% quantiles. Additionally, patches consisting of more than 95% and less than 5% building signatures were eliminated, as they were considered likely to represent erroneous detections in the segmented output.

To identify damaged buildings, we implemented a blending technique where masks from pre and post-disaster phases were merged, assigning alpha weights to control transparency. The alpha parameter is set at 0.50 for an equal blend. The resulting image, displaying damaged regions in grey, distinct from the binary black-and-white of the rest, was achieved through this blending process. Minor discrepancies in building positions between pre and post-event images, resulting from varying capture angles, caused the misidentification of undamaged buildings as small contours in the mask of the final blended images. To address this issue, a code block was developed to process the existing mask by identifying and filtering out small grey contours based on a threshold (median of contour areas). Contours below this threshold are removed from damage masks, eliminating inaccuracies and retaining highlighted areas of significant damage.

The final visual stage in the USDA-SAM approach aims to superimpose the acquired mask onto a pre-earthquake image, accentuating areas of damage. This entails a series of steps to adeptly transform and merge the images, resulting in a composite image where damaged areas are depicted in semi-transparent purple, creating a clear contrast with the original image.

For evaluating structural damages, USDA-SAM introduces the novel Damage Assessment Score (DAS) as:

$$DAS = \frac{(\mathcal{B} \triangle \mathcal{A})}{(\mathcal{B} \cap \mathcal{A})} \times \max\left(1, N_{\mathrm{b}/km^2}\right).$$

where, $\mathcal{B}$ and $\mathcal{A}$ represent binary masks corresponding to events before and after, respectively. The symbol $\triangle$ denotes the "symmetric difference," equivalent to the logical XOR operation. N_{b/km^2} indicates the

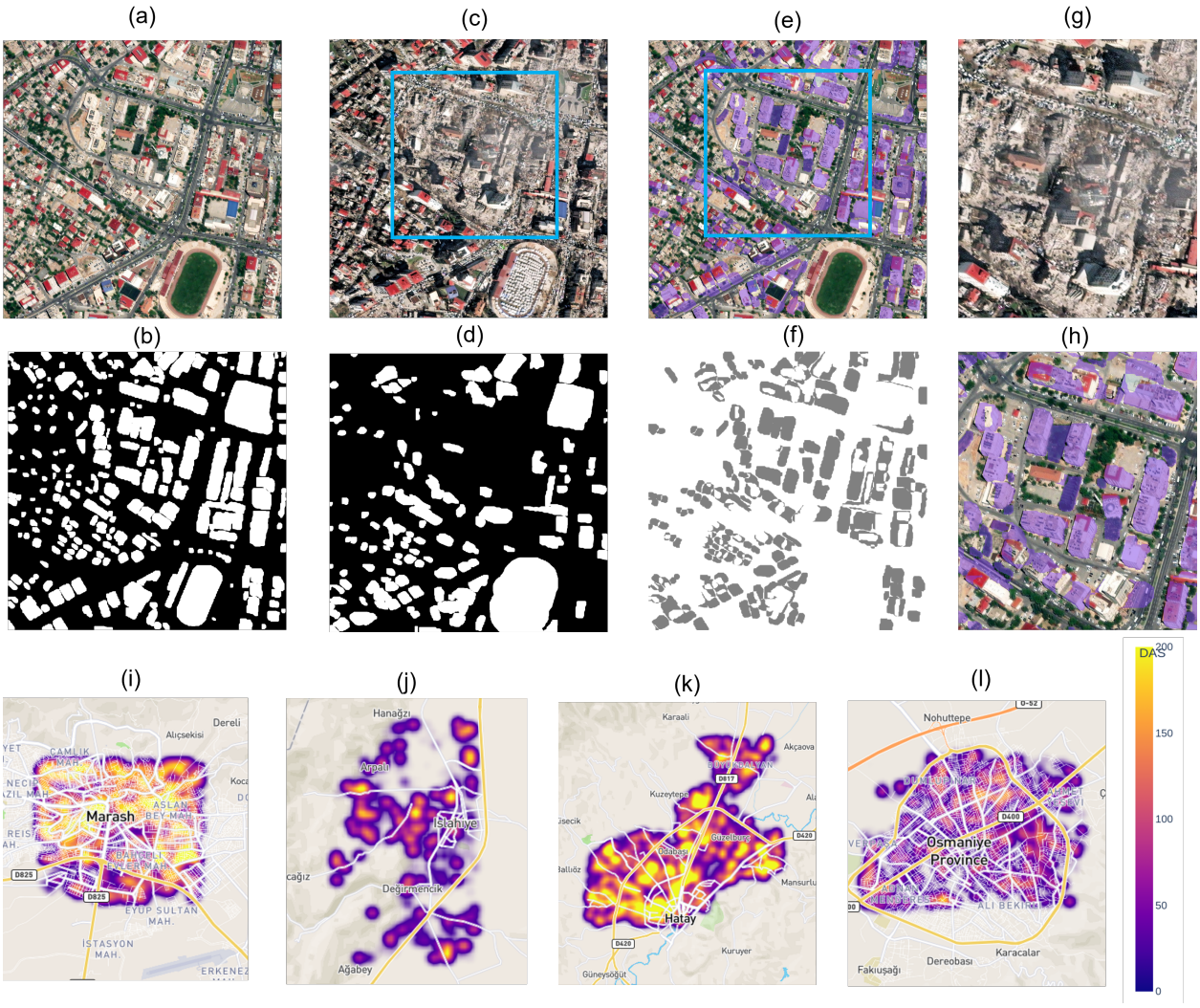

Fig. 2. Visual Building Assessment for a highly damaged region in K. Maras - 1 [(a)-(h)] and DAS density maps for all RoIs [(i)-(l)]. (a): Pre-event, (c): Post-event RGB imagery. (b) and (d) their binary masks, respectively. (e) Damage assessment map and (f) damage assessment mask. (g) and (h) are zoomed-in images of rectangles in (c) and (e), respectively. DAS density maps for K. Maras, Hatay, Islahiye and Osmaniye are shown in (i), (k), (j) and (l), respectively.

average number of affected buildings per km^2 area. In contrast to the conventional choice of a similarity score using Intersection over Union (IoU) for two binary images, DAS prioritises not only the count of buildings but also the symmetric difference between the masks, resulting in an enhanced quantification of damage assessment.

V. Experimental Analysis

In the experimental assessment detailed in this paper, we executed the USDA-SAM procedure in its entirety for all nine RoIs and gathered results comprising binary masks, Damage Assessment Masks,

Damage Assessment Maps, and quantitative Damage Assessment Score (DAS) outcomes.

Figure 2 (a)-(h) illustrates a sample visual assessment of building damage using USDA-SAM outcomes. The chosen RoI in K. Maras, significantly impacted by the earthquake, is highlighted in the zoomed-in images (g) and (h), where USDA-SAM effectively identifies the damaged region. Examining the binary masks for pre- and post-earthquake conditions in (b) and (d), it is evident that numerous buildings disappear in (d), serving as evidence that USDA-SAM successfully evaluates building damages.

TABLE I

QUANTITATIVE DAMAGE ASSESSMENT RESULTS. *ANBB: Affected number of buildings or building blocks*

Locations	IoU	N_{b/km^2}	DAS	Copernicus ANBB [27]
K.Maras - 1	0.484	36.233	108.611	927
K.Maras - 2	0.241	8.105	6.826	
Osmaniye - 1	0.248	1.637	1.255	116
Osmaniye - 2	0.512	6.679	12.131	
Islahiye - 1	0.538	3.577	12.170	33
Islahiye - 2	0.656	3.590	14.216	
Hatay - 1	0.459	8.685	85.800	593
Hatay - 2	0.662	15.312	37.547	
Hatay - 3	0.448	11.906	25.079	

Table I displays quantitative results for building damage assessment, utilizing metrics such as IoU, N_{b/km^2}, and DAS across nine RoIs. While IoU performs well in evaluating damage in relatively less affected areas like Osmaniye - 1 and K. Maras - 2, its effectiveness diminishes in highly affected regions. This limitation prompted the development of a new metric, DAS, which offers a clearer depiction of results aligned with Copernicus report [27] where K. Maras - 1 and all three Hatay regions have been dramatically affected by the earthquake. Notably, N_{b/km^2} also provides a more informative assessment compared to IoU, despite being derived simply by counting the number of building signatures in the damage assessment masks.

Figures 2 (i)-(l) depict density maps derived from DAS values for individual RoI, aligning with the data in Table I, offering insights into the devastating effect of the earthquake damage, particularly in the K. Maras and Hatay regions.

VI. Conclusion

This paper introduces an unsupervised method for evaluating structural earthquake damage, utilising the Segment Anything Model (SAM) to analyse pre and post-event remote sensing images. The proposed USDA-SAM method, by effectively comparing images and employing advanced techniques to highlight damaged areas, establishes a new benchmark for rapid and accurate damage assessment. Its notable achievement lies in the discernment and visual representation of earthquake damage, overlaying masks to spotlight affected structures, providing crucial insights for emergency response. Along with the visual analysis, proposed DAS and N_{b/km^2} metrics provided a suitable quantitative analysis. Looking forward, the integration of emerging technologies such as DeepMind's Gemini and SAM's text prompt holds great promise in enhancing these capabilities. Advanced data processing and image recognition capabilities of tools like Gemini have the potential to streamline analysis, offering even more precise and timely insights.

References

[1] A. C. Lundahl *et al.*, "Aerial photography: World class disaster fighter," *The Information Society*, vol. 3, no. 4, pp. 327–345, 1985.

[2] J. A. Boccanera, *Investigation of surface faulting, Brazoria County, Texas using aerial photography, field data, well log data, seismic profiles and fault modeling*. University of Houston, 1989.

[3] S. Yu *et al.*, "A method for rapidly determining the seismic performance of buildings based on remote-sensing imagery and its application," *Advances in Civil Engineering*, vol. 2022, 2022.

[4] M. Matsuoka *et al.*, "Characteristics of satellite images of damaged areas due to the 1995 kobe earthquake," in *Proc. of the 2nd Conf. on the Applications of Remote Sensing and GIS for Disaster Management*, 1999.

[5] A. Pachauri *et al.*, "Landslide hazard mapping based on geological attributes," *Engineering geology*, vol. 32, no. 1-2, pp. 81–100, 1992.

[6] X. Sun *et al.*, "Using insar and polsar to assess ground displacement and building damage after a seismic event: Case study of the 2021 baicheng earthquake," *Remote Sensing*, vol. 14, no. 13, p. 3009, 2022.

[7] D. Suresh *et al.*, "Insar based deformation mapping of earthquake using sentinel 1a imagery," *Geocarto International*, vol. 35, no. 5, pp. 559–568, 2020.

[8] M. Matsuoka *et al.*, "Use of satellite sar intensity imagery for detecting building areas damaged due to earthquakes," *Earthquake Spectra*, vol. 20, no. 3, pp. 975–994, 2004.

[9] S. Stramondo *et al.*, "Satellite radar and optical remote sensing for earthquake damage detection: results from different case studies," *International Journal of Remote Sensing*, vol. 27, no. 20, pp. 4433–4447, 2006.

[10] D. Brunner *et al.*, "Earthquake damage assessment of buildings using vhr optical and sar imagery," *IEEE Transactions on Geoscience and Remote Sensing*, vol. 48, no. 5, pp. 2403–2420, 2010.

[11] T. Balz *et al.*, "Building-damage detection using post-seismic high-resolution sar satellite data," *International Journal of Remote Sensing*, vol. 31, no. 13, pp. 3369–3391, 2010.

[12] A. J. Cooner *et al.*, "Detection of urban damage using remote sensing and machine learning algorithms: Revisiting the 2010 haiti earthquake," *Remote Sensing*, vol. 8, no. 10, p. 868, 2016.

[13] J. Bialas *et al.*, "Object-based classification of earthquake damage from high-resolution optical imagery using machine learning," *Journal of Applied Remote Sensing*, vol. 10, no. 3, pp. 036 025–036 025, 2016.

[14] S. Naito *et al.*, "Building-damage detection method based on machine learning utilizing aerial photographs of the kumamoto earthquake," *Earthquake Spectra*, vol. 36, no. 3, pp. 1166–1187, 2020.

[15] T. Miyamoto *et al.*, "Using multimodal learning model for earthquake damage detection based on optical satellite imagery and structural attributes," in *IGARSS 2020-2020 IEEE International Geoscience and Remote Sensing Symposium*. IEEE, 2020, pp. 6623–6626.

[16] B. Adriano *et al.*, "Learning from multimodal and multitemporal earth observation data for building damage mapping," *ISPRS Journal of Photogrammetry and Remote Sensing*, vol. 175, pp. 132–143, 2021.

[17] K. Hacıefendioğlu *et al.*, "Automatic detection of earthquake-induced ground failure effects through faster r-cnn deep learning-based object detection using satellite images," *Natural Hazards*, vol. 105, pp. 383–403, 2021.

[18] R. Virtriana *et al.*, "Machine learning remote sensing using the random forest classifier to detect the building damage caused by the anak krakatau volcano tsunami," *Geomatics, Natural Hazards and Risk*, vol. 14, no. 1, pp. 28–51, 2023.

[19] A. Kirillov *et al.*, "Segment anything," *arXiv:2304.02643*, 2023.

[20] Y. Huang *et al.*, "Segment anything model for medical images?" *Medical Image Analysis*, p. 103061, 2023.

[21] M. A. Mazurowski *et al.*, "Segment anything model for medical image analysis: an experimental study," *Medical Image Analysis*, vol. 89, p. 102918, 2023.

[22] L. P. Osco *et al.*, "The segment anything model (sam) for remote sensing applications: From zero to one shot," *International Journal of Applied Earth Observation and Geoinformation*, vol. 124, p. 103540, 2023.

[23] S. Ren *et al.*, "Segment anything, from space?" in *Proceedings of the IEEE/CVF Winter Conference on Applications of Computer Vision*, 2024, pp. 8355–8365.

[24] Maxar-Technologies, "Turkey earthquake 2023," 2023. [Online]. Available: https://www.maxar.com/open-data/turkey-earthquake-2023

[25] Q. Wu *et al.*, "samgeo: A Python package for segmenting geospatial data with the Segment Anything Model (SAM)," *Journal of Open Source Software*, vol. 8, no. 89, p. 5663, 2023.

[26] X. Zhao *et al.*, "Fast segment anything," *arXiv:2306.12156*, 2023.

[27] Copernicus EMSR, "Report Of Activation On Earthquake Event In East Anatolian Fault Zone, Republic Of Turkiye - EMSR648," *Copernicus*, 2023. [Online]. Available: https://emergency.copernicus.eu/mapping/list-of-components/EMSR648